



MANAR MOHAMMED ALI AHMED EDRIS İSTANBUL ÜNİVERSİTESİ SAĞ.BİL.ENST. YÜKSEK LİSANS TEZİ İSTANBUL-2025



TC

İSTANBUL ÜNİVERSİTESİ
SAĞLIK BİLİMLERİ ENSTİTÜSÜ
(MASTER THESIS)

**STANDARDIZED SURGICAL GUIDE FOR PROXIMAL FEMORAL
OSTEOTOMY**

MANAR MOHAMMED ALI AHMED EDRIS

SUPERVISOR

PROF. DR. FUAT BİLGİLİ

**ORTHOPEDECS AND TRAUMATOLOGY / ORTHOPEDIC AND
BIOMEDICAL NEUROTHECNOLOGY**

İSTANBUL-2025

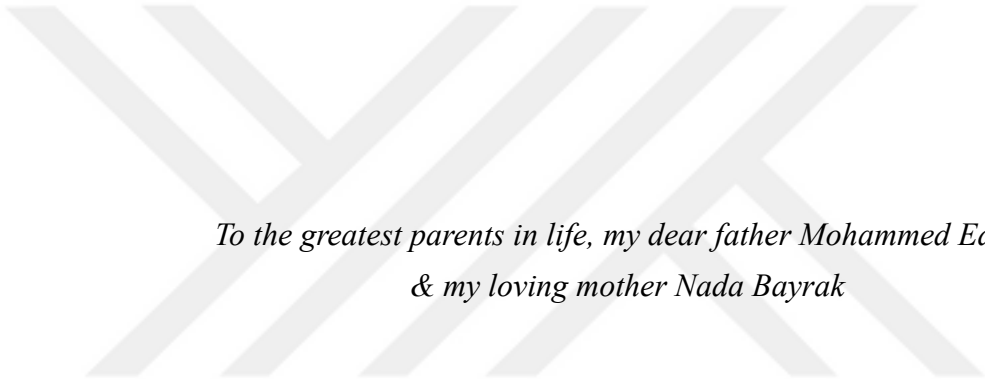
DECLARATION

This thesis is my work, I have not acted dishonestly at all stages from the scheduling to the writing of the thesis, I have acquired all the data presented in this thesis in accordance with academic and ethical guidelines. The proper citations have been provided for all external information and opinions not originating from this study, and these sources are duly listed in the references section. It is hereby confirmed that no infraction of patents or copyrights has occurred during the research and composition of this thesis.

Manar Mohammed Alı Ahmed Edris



DEDICATION



*To the greatest parents in life, my dear father Mohammed Edres
& my loving mother Nada Bayrak*

ACKNOWLEDGMENT

First and foremost, my heartfelt thanks go to my fiancé Faruk who has been my source of strength throughout this journey. Thank you for always being there and making this journey easier. Thank you for your immense patience and support.

This thesis would not have been possible without the guidance and support of my advisors. I would like to express my sincere gratitude to my esteemed advisor, Prof.Dr. Fuat Bilgili, for his insightful contributions, constructive feedback, and both academic and personal support throughout every stage of this work. I also wish to extend my heartfelt thanks to my advisor Prof.Dr. Hayati Durmaz for his continuous guidance and encouragement, His valuable input has greatly enriched the quality of this thesis, and I am truly grateful.

Finally, I would like to acknowledge all those who, directly or indirectly, contributed to the realization of this work. In particular, I would like to thank Dr. Yavuz Sağlam and the Ortovizyon Company for generously providing the surgical set used in the experiments and all the assistants help me to make this work.

CONTENTS

| | |
|--|-------------------------------------|
| DEDICATION | i |
| ACKNOWLEDGMENT..... | iii |
| CONTENTS..... | iv |
| LIST OF TABLES | v |
| LIST OF FIGURES | vi |
| ABBREVIATIONS..... | vii |
| ABSTRACT..... | viii |
| ÖZET | ix |
| 1. INTRODUCTION | 1 |
| 2. BACKGROUND AND LITERATURE REVIEW | 3 |
| 2.1. Hip Development and Anatomy | 3 |
| 2.3. Paediatric Femoral Osteotomy: Indications and Technique | 4 |
| 2.3.1. Varus Osteotomy | 5 |
| 2.3.2. Valgus Osteotomy..... | 6 |
| 2.3.3. Pauwells "Y" Osteotomy | 6 |
| 2.4. Preoperative Planning..... | 7 |
| 2.5. Surgical Guides: Traditional vs. 3D-Printed Solutions | 8 |
| 2.6. 3D Printing Materials and Technologies | 9 |
| 2.7. Application of 3D-Printing in Orthopaedic | 12 |
| 3. METHODOLOGY..... | 17 |
| 3.1 Surgical Guide Designing..... | 17 |
| 3.2. Guide 3D Printing..... | 20 |
| 3.3. Surgical Procedure..... | 21 |
| 4. RESULTS..... | 24 |
| 5. DISCUSSION | 27 |
| 6. CONCLUSION AND FUTURE STUDIES | 31 |
| REFERENCES..... | 32 |
| FORMS | Error! Bookmark not defined. |
| THE FIRST PAGE OF THE PLAGIARISMREPORT..... | 37 |

LIST OF TABLES

| | |
|--|----|
| Table 2. 1. 3D printing techniques..... | 11 |
| Table 3. 1. Preoperative planning and LCP plate selection for experimental cases | 23 |
| Table 4. 1. Preoperative deformity and postoperative residual error..... | 25 |



LIST OF FIGURES

| | |
|--|----|
| Figure 2. 1. Normal hip joint..... | 4 |
| Figure 2. 2. Development of Neck-Shaft Angle..... | 4 |
| Figure 2. 3. Femoral neck anteversion and retroversion..... | 4 |
| Figure 2. 4. Varus correction with LCP hip plate..... | 5 |
| Figure 2. 5. Pauwells "Y" osteotomy..... | 7 |
| Figure 2. 6. Schematic diagram of an IGOS system..... | 9 |
| Figure 2. 7. 3D-Printing Workflow..... | 12 |
| Figure 3. 1. Concept diagram of the hybrid design approach..... | 17 |
| Figure 3. 2. Initial design of the guide..... | 18 |
| Figure 3. 3. Revised surgical guide model..... | 19 |
| Figure 3. 4. 3D printed prototype surgical guide..... | 20 |
| Figure 3. 5. Femur models..... | 21 |
| Figure 3. 6. Simulation of the guide on femur bone..... | 22 |
| Figure 4. 1. Procedural duration and K-wire usage across trials..... | 26 |

ABBREVIATIONS

PFO: Proximal Femoral Osteotomy

AM: Additive Manufacturing

FDM: Fused Deposition Modeling

SLA: Stereolithography

PSI: Patient-Specific Instruments

CAD: Computer Aided Design

PLA: Polylactic Acid

NSA: Neck-Shaft Angle

AV: Anteversion Angle

LCP: Locking Compression Plate

IGOS: Image-Guided Orthopaedic Surgery

PSGS: Patient-Specific Guides

VSS: Visually Simulated Surgery

ROM: Range Of Motion

ABSTRACT

Edris, M. (2025), Standardized Surgical Guide For Proximal Femoral Osteotomy. Istanbul University, Health Sciences Institute, Department of Orthopedic and Biomedical Neurotechnology, Master's Thesis, Istanbul.

This study aimed to develop and evaluate a 3D-printed standardized surgical guide for pediatric proximal femoral osteotomy, focusing on accuracy, usability, and efficiency. The guide was designed with consideration of mechanical feasibility, anatomical adaptation, and surgical applicability, and fabricated using fused deposition modeling (FDM) with polylactic acid (PLA). Experiments were conducted on five composite femoral models at the Department of Orthopedics and Traumatology, Istanbul University, by surgeons with varying levels of experience. Planned corrections of femoral anteversion and neck–shaft angle were compared with achieved postoperative outcomes, while operative time and learning curve were assessed as secondary parameters. Postoperative alignment showed high accuracy, with mean deviations of $1.26^{\circ} \pm 0.80$ for angulation and $0.94^{\circ} \pm 0.93$ for rotation. Usability testing through structured questionnaires yielded favorable evaluations, with surgeons rating overall functionality at 4.6 ± 0.89 and accuracy of correction at 4.2 ± 0.45 . The mean time required per Kirschner wire was 1.8 minutes, with no major differences observed between trials or surgeon experience levels, indicating a short learning curve and ease of adoption. These findings demonstrate that the proposed guide provides accurate, reproducible, and efficient performance in simulated osteotomies, supporting its potential application in pediatric orthopaedic surgery. Further validation with anatomical specimens and clinical trials is recommended to confirm reproducibility across diverse femoral morphologies

Keywords: Proximal femoral osteotomy, surgical guide, 3D printing, angulation, rotation.

ÖZET

Edris, M. (2025). Proksimal Femor Osteotomi İçin Standartlaştırılmış Cerrahi Kılavuz. İstanbul Üniversitesi, Sağlık Bilimleri Enstitüsü, Ortopedi ve Biyomedikal Nöroteknoloji ABD, Yüksek Lisans Tezi. İstanbul.

Bu çalışmanın amacı, doğruluk, kullanılabilirlik ve verimliliğe odaklanarak pediatrik proksimal femoral osteotomi için 3 boyutlu yazdırılmış standart bir cerrahi kılavuz geliştirmek ve değerlendirmektir. Kılavuz, mekanik uygulanabilirlik, anatomik adaptasyon ve cerrahi uygulanabilirlik göz önünde bulundurularak tasarlanmış ve polilaktik asit (PLA) ile füzyon biriktirme modellemesi (FDM) kullanılarak üretilmiştir. Deneyler, İstanbul Üniversitesi Ortopedi ve Travmatoloji Anabilim Dalı'nda farklı deneyim seviyelerine sahip cerrahlar tarafından beş kompozit femoral model üzerinde gerçekleştirilmiştir. Femoral anteversiyon ve boyun-şaft açısının planlanan düzeltmeleri, elde edilen postoperatif sonuçlarla karşılaştırılırken, operasyon süresi ve öğrenme eğrisi ikincil parametreler olarak değerlendirildi. Ameliyat sonrası hizalama, angülasyon için $1.26^{\circ} \pm 0.80$ ve rotasyon için $0.94^{\circ} \pm 0.93$ ortalama sapmalarla yüksek doğruluk gösterdi. Anketler aracılığıyla yapılan kullanılabilirlik testleri, cerrahların genel işlevselliği 4.6 ± 0.89 ve düzeltme doğruluğunu 4.2 ± 0.45 olarak derecelendirmesiyle olumlu değerlendirmeler sağladı. Kirschner teli başına gereken ortalama süre 1.8 dakika olup, denemeler veya cerrah deneyim seviyeleri arasında önemli bir fark gözlenmemiştir; bu da kısa bir öğrenme eğrisi ve kolay benimsenme anlamına gelmektedir. Bu bulgular, önerilen kılavuzun simüle edilmiş osteotomilerde doğru, tekrarlanabilir ve verimli bir performans sağladığını ve pediatrik ortopedik cerrahideki potansiyel uygulamasını desteklediğini göstermektedir. Çeşitli femoral morfolojilerde tekrarlanabilirliği doğrulamak için anatomik örnekler ve klinik çalışmalarla daha fazla doğrulama önerilmektedir.

Anahtar Kelimeler: Proksimal femoral osteotomi, cerrahi kılavuz, 3D baskı, angülasyon, rotasyon

1. INTRODUCTION

In addressing hip misalignment in children, such as developmental dysplasia of the hip (DDH), slipped capital femoral epiphysis (SCFE), and Perthes disease, surgical intervention is recognized as fundamental when conservative strategies fail. The primary goal of surgical procedures is to achieve stable alignment of the hip joint in order to restore its functionality, thereby promoting proper development of the hip joint, while minimizing the risk of osteonecrosis and reducing the need for additional corrective procedures (1). Proximal femoral osteotomy is one of the principal surgical methods used to correct femoral deformities, particularly in skeletally immature patients. The objective of this surgical procedure is to restore hip alignment, enhance the distribution of mechanical loads, and preserve the mobility of the joint (2). Successful correction of femoral deformities requires precise realignment at multiple levels, including varus/valgus angulation, femoral anteversion (rotation), and translational positioning. These parameters are highly sensitive and can be affected by changes during the procedure, which can lead to variability in results and the potential for postoperative complications (3). Conventional osteotomy techniques typically rely on intraoperative estimation, fluoroscopic guidance, and the surgeon's experience. Although these methods may achieve acceptable outcomes, they remain subject to errors, often lead to prolonged operative times, and increase radiation exposure for both patients and surgical staff (4).

In recent years, patient-specific instruments (PSI) and computer-aided design (CAD) combined with 3D printing have emerged as promising tools for enhancing surgical accuracy and reproducibility. These technologies allow preoperative planning to be translated directly into customized guides, reducing reliance on intraoperative estimation and potentially minimizing errors, operative time, and radiation exposure. However, several challenges, including the high cost, complex manufacturing processes, and lengthy production times associated with fully customized guides have limited their routine application, particularly in paediatric cases where ongoing growth and anatomical variability present additional constraints. Nevertheless, these advancements represent a significant step toward more precise and individualized surgical care and provide a foundation for further research aimed at optimizing guide design, usability, and clinical applicability (5).

Building on this progress, the aim of this pilot study is to develop and evaluate a 3D-printed standardized surgical guide for pediatric proximal femoral osteotomy with the potential to achieve correction accuracy comparable to that reported for PSI. The proposed guide is intended to provide high accuracy and reproducibility in correcting deformities while ensuring broad applicability to diverse morphologies. In addition, it is designed to overcome the limitations of PSI by offering cost-efficiency, reusability, and reduced manufacturing complexity and lead time, thereby combining the precision of customized devices with the practicality required for routine clinical use.

This study hypothesizes that a standardized 3D-printed surgical guide can achieve rotation and angulation with high accuracy, while also reducing preparation time and improving usability across multiple cases. The core research questions are

- Can the standardized guide achieve accurate correction of femoral anteversion and neck–shaft angle (NSA) comparable to ranges reported for PSI?
- Can the same guide be applied reproducibly across different paediatric femoral morphologies?
- Can less experience assistance surgeon use the device with confidence and high accuracy
- Does the guide reduce overall preparation and intraoperative time?
- How does the guide perform in terms of ergonomics and ease of use?

This pilot study lay the foundation for the development of a clinically adaptable and reusable surgical guide specifically designed to meet the unique needs of paediatric proximal femoral osteotomy. By integrating surgeon feedback, benefit current manufacturing techniques, and validating the device through anatomically accurate simulations, this research aims to bridge the gap between patient-specific accuracy and practicality of standardized solutions. The following sections will provide a comprehensive review of the anatomical, clinical, and technological background underlying this project, followed by detailed methodology and results, and a discussion of the surgical guide design and evaluation process.

2. BACKGROUND AND LITERATURE REVIEW

2.1. Hip Development and Anatomy

The human hip joint begins to develop early in fetal life and undergoes continuous morphological changes throughout development. The femoral head and acetabulum start to develop as cartilaginous structures in the seventh week of gestation, while primary ossification of the femoral shaft begins by the eighth week. The vascular supply of the proximal femur is well established between the 12th and 14th weeks, laying the foundation for the subsequent development of the femoral head and neck (Figure 2.1.) (6).

The geometry of the proximal femur is determined by the neck-Shaft angle (NSA) and femoral anteversion (AV). The neck shaft angle is 145 degrees in mid-pregnancy and gradually decreases to 125 degrees by puberty (Figure 2.2.). Similarly, the average femoral anteversion angle is approximately 45 degrees at birth (Figure 2.3.; 7;8). These developmental changes reflect the femur's adaptation to mechanical loading requirements and are essential for understanding the pathogenesis and surgical correction of pediatric hip deformities (7; 9).

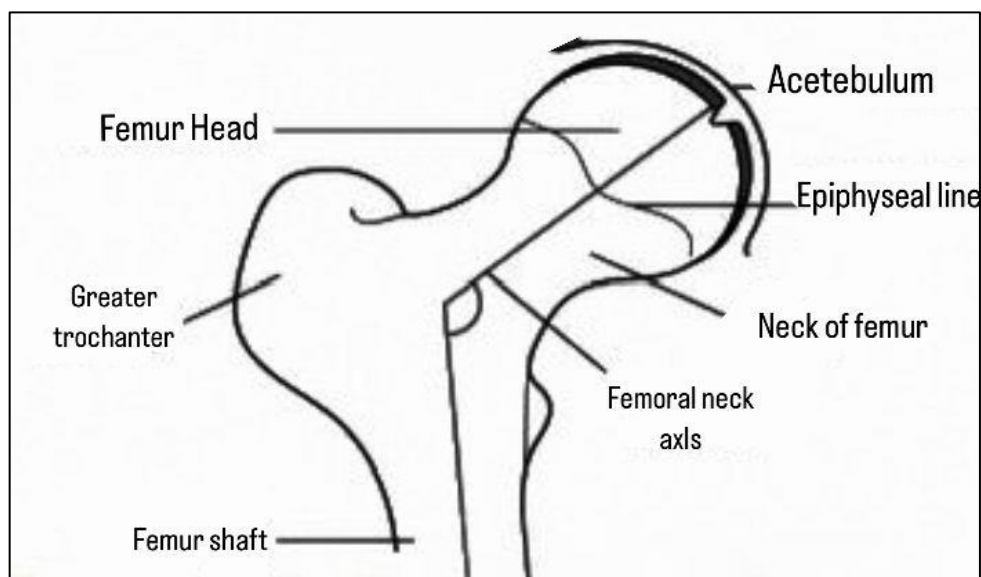


Figure 2.1. Normal hip joint

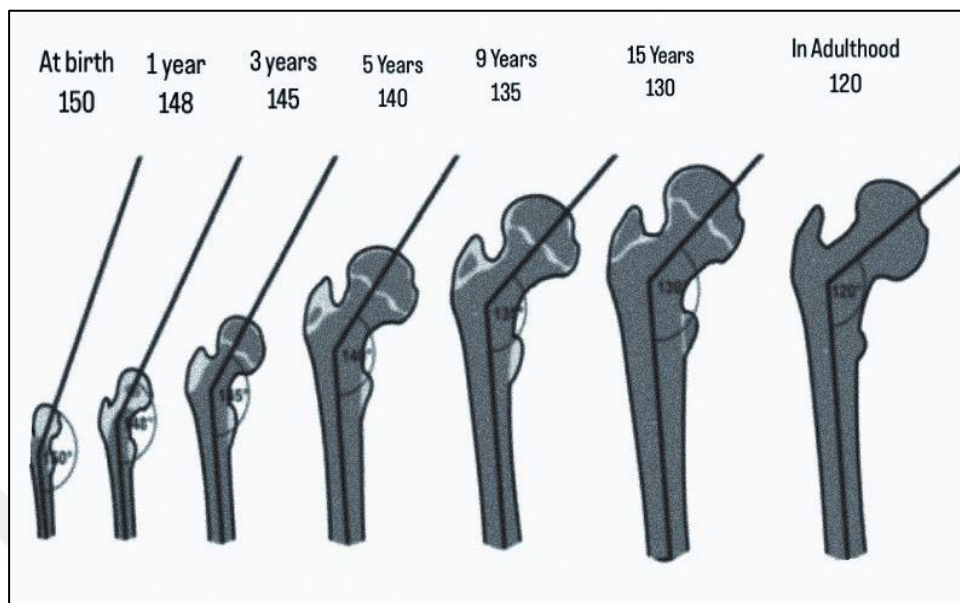


Figure 2. 1. Development of Neck-Shaft Angle

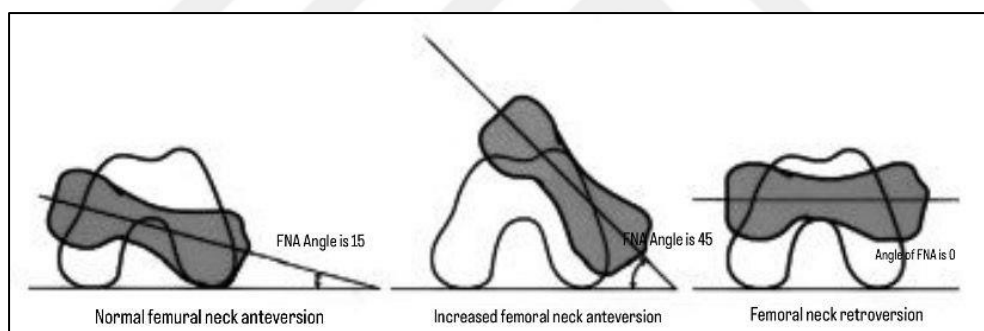


Figure 2. 2. Femoral neck anteversion and retroversion

2.3. Paediatric Femoral Osteotomy: Indications and Technique

Femoral osteotomy in children is an important surgical procedure used to correct deformities in the upper femur. It plays an important role in improving hip function and preventing joint erosion in younger patients. This procedure is commonly used to manage conditions such as developmental dysplasia of the hip (DDH), Legg-Calve-Perthes disease, and slipped capital femoral epiphysis (SCFE). This procedure effectively corrects structural problems that can disrupt normal hip function and lead to movement restrictions. By realigning the femoral head and neck, it relieves discomfort and improves hip stability (10). There are two common types of osteotomies: intertrochanteric osteotomy (which treats varus, flexion, and extension) and greater intertrochanteric

osteotomy. Intertrochanteric osteotomy is often preferred for specific hip deformities due to its proximity to the joint, rapid healing, and lower risk of vascular injury.

Intertrochanteric osteotomies require careful preoperative planning, often guided by clinical examination and advanced imaging, to ensure optimal hip alignment. Imaging techniques, such as x-rays and diagnostic arthroscopy, are used to help positioning of the femoral head within the acetabulum and to help identify potential femoral impingement. The patient is usually positioned in the lateral or dorsal position during surgery. The procedure starts with an incision approximately 8-10 cm long made at the apex of the greater trochanter, and the osteotomy is performed perpendicular to the femoral shaft from the lesser trochanter (11;12).

2.3.1. Varus Osteotomy

Varus correction can be performed with a locking compression plate (LCP) using two main approaches. In the fixed-angle method, guide wires and proximal screws are placed parallel to the femoral neck axis. In the calculated-angle technique, specialized instruments determine the optimal entry point and screw placement according to the plate angle and planned correction. For instance, to correct 25° varus using 110° plate it requires to set the instruments at 135°. Once fixation is achieved, the osteotomy is completed and the fragments realigned before distal fixation (Figure 2.4.) (12).



Figure 2. 3. Varus correction with LCP hip plate [Coll. J.M. Clavert]. Reproduced with permission from Louahem M'sabah D, Assi C, Cottalorda J. Proximal femoral osteotomies in children. *Orthop Traumatol Surg Res.* 2013;99(Suppl 1):S171–S186. © Elsevier

2.3.2. Valgus Osteotomy

The procedure follows similar principles to varus correction but is adapted to achieve valgus realignment. The neck–shaft angle (NSA) is measured and compared with the target NSA to determine the required correction. The LCP is selected based on the desired NSA. The entrance angle for the first guide wire with respect to the femoral shaft axis on the anteroposterior (AP) plane is then determined by subtracting the correction angle from the plate angle. Guide wires are introduced along the femoral neck under fluoroscopic guidance to establish anteversion and provide a reliable rotational reference. Once the proximal screws are placed into the femoral head and neck at the calculated orientation, a lateral closing or opening wedge osteotomy is performed at the intertrochanteric level. The proximal and distal parts are realigned to achieve the planned correction, and the plate is fixed distally with cortical or locking screws (12).

2.3.3. Pauwells "Y" Osteotomy

Powles osteotomy is primarily recommended in cases with significant lateral curvature of the femur (Figure 2.5A). The process entails resecting an intertrochanteric wedge in accordance with the necessary corrective angle; for instance, a wedge of 44° would be needed for a hip–epiphyseal (HE) angle of 60° ($60^\circ - 16^\circ = 44^\circ$). If necessary, the femur is realigned prior to resection to ensure accuracy (Figure 2.5B). Two guide pins are used to define the wedge: one is positioned obliquely above the lateral cortex toward the first pin, and the other is positioned horizontally beneath the greater trochanter, thus creating the osteotomy plane (Figure 5C). After the wedge is removed, the osteotomy is completed medially, and correction is performed by shifting the proximal portion laterally and inferiorly while abducting the distal portion of the femur (Figure 2.5D). The bone is usually stabilized with a curved plate and the femoral neck is fixed with at least two screws. In younger children, stabilization may instead be achieved using two pins reinforced with a tension band (12;13).

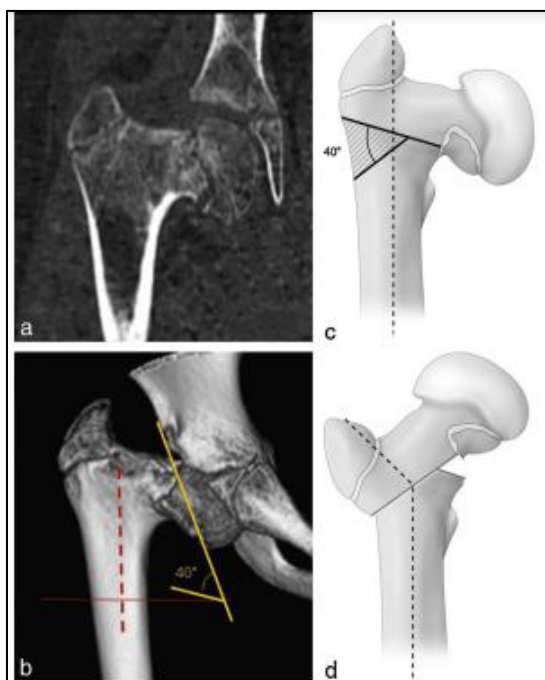


Figure 2. 4. Pauwells "Y" osteotomy. Reproduced with permission from Louahem M'sabah D, Assi C, Cottalorda J. Proximal femoral osteotomies in children. *Orthop Traumatol Surg Res.* 2013;99(Suppl):S171-S186. © Elsevier.

2.4. Preoperative Planning

Planning before surgery is a decisive step in the management of complex femoral deformities. The process usually begins with conventional radiographic evaluation. A standing anteroposterior (AP) pelvis X-ray with the hips in neutral rotation, together with AP and lateral views of the femur, are commonly obtained. These images provide essential details on limb alignment, the mechanical axis, and joint morphology, all of which are necessary to guide a precise correction strategy (14). Recently, the accuracy of preoperative planning has been markedly improved by digital tools. Three-dimensional (3D) reconstruction and computer-aided design (CAD) programs allow the surgeon to visualise deformities in much greater detail. Virtual simulation of surgery (VSS) has added further value by permitting osteotomy cuts and correction angles to be tested on a digital model before entering the operating room. The main benefits of these methods are increased precision, a reduction in intraoperative fluoroscopy, and shorter overall operative times (15).

Equally important is the adoption of a structured and reproducible planning approach. The use of physical and digital templates helps the surgeon to predetermine osteotomy levels, correction angles, and fixation options (14;16).

2.5. Surgical Guides: Traditional vs. 3D-Printed Solutions

Orthopaedic surgery is known for its difficulty due to the complexity of the anatomical structures and surgical techniques. These surgeries carry big risks due to the dense structure of soft tissues and nerves surrounding the surgical site. The limited field of vision and poor visibility of the surgical site further complicated these procedures. Traditional surgical instruments play a vital role in orthopaedic procedures, helping surgeons achieve precise positioning, and alignment. These instruments ensure consistent osteotomy and bone alignment, contributing to reduced variability in surgical outcomes. Historically, as Otani notes in his study, manual surgical methodologies that mostly depended on the surgeon's expertise and knowledge of anatomical structures often produced variable outcomes due to the possibility of human error. These errors were often related to problems such as saw blade movement or instability of surgical instruments (17).

The use of metal templates and alignment tools has increased the stability of precise angles during surgery. However, they show some limitations such as increased surgical time, prolonged recovery times, and inability to adapt to individual patient anatomical differences (18). Radiographic templates provide intraoperative guidance using two-dimensional imaging, but they do not reflect the complexity of three-dimensional anatomical structures. Although traditional tools have been important in orthopaedic surgery for decades, they are often insufficient for complex cases or those requiring precise anatomy. Surgical guides, general and patient-specific, have emerged as solutions that significantly improve surgical accuracy. These guides address the limitations of traditional methods by providing specific reference points that improve alignment and reduce variability, especially in complex procedures (19).

Image-guided orthopaedic surgery (IGOS) shows a great role in improving surgical outcomes and reduced risks by optimizing both preoperative planning and intraoperative procedures. By providing detailed segmentation related anatomical structures from medical imaging IGOS systems help in precise surgical preparation in the preoperative phase. During surgery, these systems provide real-time guidance by

monitoring the position and orientation of surgical instruments relative to the patient using image registration instruments. However, the high financial investment required to purchase and install the systems and the significant time required for preoperative preparation limit their accessibility. In addition, the complexity of these systems requires advanced expertise and extensive training for surgeons, highlighting the importance of more user-friendly solutions. (20) (Figure 2.6.).

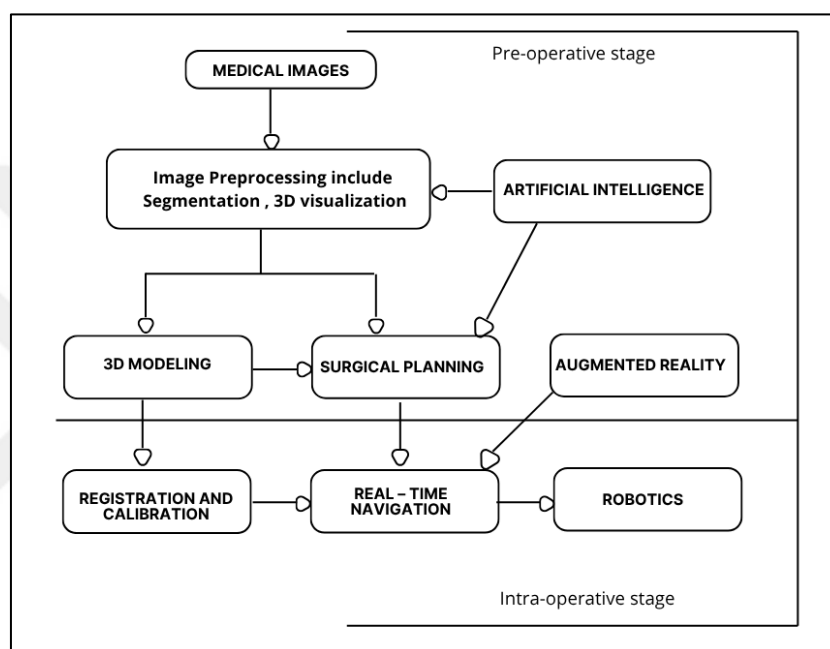


Figure 2. 5. Schematic diagram of an IGOS system and its pre-operative and intra-operative components

2.6. 3D Printing Materials and Technologies

3D printing, also known as additive manufacturing, is an advanced technology that produces materials layer by layer from digital data. In the medical field, it has emerged as an effective tool for overcoming the challenges of traditional surgical procedures, especially in cases requiring high precision and patient-specific solutions. 3D printing has facilitated the development of surgical guides.

Orthopaedic has been at the forefront of integrating 3D printing in medical, using it extensively in surgical planning, medical education, personalized device design, and navigation template design. These advancements have revolutionized the accuracy of surgical procedures and enhanced both clinical outcomes and the training of surgeons (21;22).

The table below highlights various 3D printing techniques, their advantages, and applications, focusing on materials used and their role in advancing surgical navigation solutions (Table 2.1.) (23;24).



Table 2. 1. 3D printing techniques

| TECHNOLOGIES | TECHNIQUES | MATERIALS | APPLICATION | ADVANTAGES | DESADVANTAGES |
|--|--|--|---|--|---|
| <p>Stereolithography (SLA)</p> <p>Digital light processing (DPL)</p> | <p>Vat polymerization uses a vat of liquid photopolymer resin, out of which the model is constructed layer by layer</p> | <p>-Photopolymer resin</p> | <p>Bone</p> | <p>-High resolution and accuracy</p> <p>-Complex parts</p> <p>-Decent surface finish and smoother finish</p> <p>-Flexible printing setup</p> | <p>-Lacking in strength and durability</p> <p>-Still affected by UV light after print</p> <p>-Not for heavy use</p> |
| <p>Fused deposition modelling (FDM)</p> <p>Fused filament fabrication (FFF)</p> | <p>Fused Deposition Modeling involves feeding material through a heated nozzle. The nozzle deposits the material layer by layer, moving horizontally, while the build platform adjusts vertically after each layer is completed.</p> | <p>- Plastics; - Polymers: ABS, nylon, PC, AB</p> | <p>Medical instruments and devices, rapid prototyping exoskeleton</p> | <p>-Inexpensive process</p> <p>-Widespread</p> <p>-ABS plastic supported: good structural properties and easily accessible</p> | <p>-Dependence of quality on the nozzle radius: bigger nozzle leads to less quality</p> <p>-Low accuracy and dependence on the nozzle thickness</p> <p>-Low speed</p> |
| <p>Selective laser sintering (SLS)</p> <p>Direct metal laser sintering (DMLS)</p> <p>Selective heat sintering (SHS)</p> <p>Selective laser melting (SLM)</p> <p>Electron beam melting (EBM)</p> | <p>The powder bed fusion process includes the following commonly used printing techniques: direct metal laser sintering (DMLS), electron beam melting (EBM), selective heat sintering (SHS), selective laser melting (SLM) and selective laser sintering (SLS)</p> | <p>-Powder-based materials. Common metals and polymers used are (i) SHS: nylon DMLS, SLS, SLM:stainless steel, titanium, aluminium, cobalt chrome, steel</p> <p>EBM: titanium, cobalt chrome, stainless steel material, aluminium and copper</p> | <p>Medical devices</p> | <p>-Inexpensive</p> <p>-Small technology: office size machine</p> <p>-Large range of material options</p> | <p>-Low speed</p> <p>-Limited sizes</p> <p>-Dependence on powder grain size</p> |
| <p>Laminated object manufacturing (LOM)</p> <p>Ultrasonic consolidation (UC)</p> | <p>Sheet lamination techniques processes like Ultrasonic Additive Manufacturing (UAM) and Laminated Object Manufacturing (LOM). UAM specifically employs sheets or ribbons of metal that are fused together through ultrasonic welding.</p> | <p>-Paper</p> <p>-plastic</p> <p>-sheet metals</p> | <p>Orthopaedic modelling of bone surfaces</p> | <p>-Speed</p> <p>-Inexpensive</p> <p>-Ease of materials handling</p> | <p>-Need of postprocessing</p> <p>-Limited material range</p> |

2.7. Application of 3D-Printing in Orthopaedic

3D printing plays a great role in enhancing both preoperative planning and intraoperative execution. By converting medical imaging data into anatomically accurate models, patient-specific instruments (PSIs), or navigation guides, 3D printing enables surgeons to visualise complex deformities, simulate procedures, and design tailored surgical solutions.

Creating a 3D-printed *surgical model* involves five basic technical steps. First, the target region is identified based on medical imaging from CT scans or MRIs. These images are then processed to develop the geometry of the 3D model. The digital file is optimized for printing, after which a 3D printer and appropriate materials are selected. The final step involves sectioning the digital design into sectional layers, allowing the printer to produce the model layer by layer using the selected raw materials (Figure 2.7.). This process produces a patient-specific, anatomically accurate model derived from the imaging dataset (24).

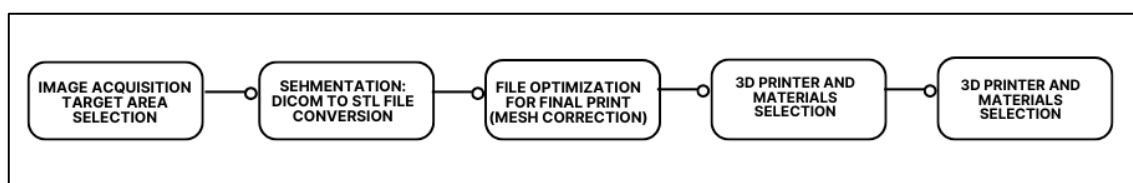


Figure 2. 6. 3D-Printing Workflow

These surgical models have important applications in preoperative planning by allowing surgeons to examine anatomy, understand abnormalities, and perform surgical procedures, improving accuracy and reducing intraoperative uncertainty (25). Furthermore, surgical models are also useful during surgery, assisting with tasks such as bending plates to treat fractures and used as a reference to verify anatomical landmarks, thus ensuring the accuracy of surgical interventions (24).

The Development of patient-specific guides (PSGs) for orthopaedic surgery involves several key steps. The process begins with preoperative planning, where a surgical plan is created based on the patient's unique anatomy using accurate imaging and

modeling. Following this, the guide design phase uses computer-aided design (CAD) software to create a device that aligns perfectly with the patient's anatomy. Once designed, the PSG is usually manufactured using 3D printing. Before surgery, the PSG undergoes validation to verify that it meets all specifications and functions correctly according to the preoperative plan. Finally, during the procedure, the PSG is implemented in strict accordance with the surgical plan, with any deviations considered an error that must be addressed (26).

The literature on the use of surgical guides in femoral osteotomy has been extensively researched, highlighting their potential for improving surgical precision and outcomes. For example, a study by Sun et al. illustrates the challenges faced by orthopaedic surgery in children with developmental dysplasia of the hip (DDH), particularly in terms of the complexity of proximal femoral deformities. The study aimed to evaluate the effectiveness of 3D-printed osteotomy guide plates in femoral osteotomy by comparing their clinical outcomes with those obtained using conventional methods. The research involved an examination of medical records of young patients who had Salter osteotomy and open reduction combined with femoral osteotomy over a decade. A total of 36 patients were analysed and divided into two groups: one treated with 3D-printed guide plates and the other using conventional surgical techniques. Three key performance indicators were evaluated in the study: operative time, number of fluoroscopy exposures, and intraoperative blood loss. The results showed significant advantages in the group that used 3D printing guides, such as shorter operation time and less blood loss, while no significant difference was observed in post-operative outcomes between the two groups (27).

Another study by Cheng et al. examined the use of a 3D-printed navigation template for osteotomy for proximal femoral varus and shortening in older children with developmental dysplasia of the hip (DDH). The study included 12 patients who underwent surgery using a navigation template and 13 patients who underwent a traditional surgical approach. The results showed that the template-guided group had reduced operative time (21.08 minutes versus 46.92 minutes) and fewer hips were resected. Follow-up assessments conducted between 12 and 18 months after surgery indicated that 66.7% of hips in the template-guided group rated as excellent or good based on the Mackay standards, and 83.3% received comparable assessments based

on the Severin standards. While the results in the group using templates were better, the variations were not statistically significant. Overall, the study highlights the potential of the navigation template to simplify the procedure, increase accuracy, and reduce surgical risks in children with myelodysplasia (28).

Qiang Shi and Deyi Sun's study aimed to assess the effectiveness and safety of a novel personalized navigation template in performing proximal femoral corrective osteotomy for DDH. The study included 29 patients, with 15 undergoing surgeries using a navigation template and 14 treated with the conventional approach. Results showed that the navigation template group had no major complications, such as redislocation or avascular necrosis, and achieved higher accuracy in osteotomy angles, along with reduced radiation exposure and shorter operative times compared to the conventional group ($P < 0.05$). Moreover, the navigation template group showed significantly better outcomes based on the McKay criteria ($P = 0.0362$). The study highlights the potential of personalized navigation templates to improve surgical precision and safety in osteotomy procedures for DDH, offering improved patient outcomes and reducing the risks associated with traditional surgical techniques (29).

Furthermore, Ballard et al. study assesses the financial advantages of using 3D-printed anatomic models and surgical guides in orthopaedic and maxillofacial surgeries, specifically their potential to lower operating room (OR) costs by reducing procedure times. A comprehensive literature review identified seven studies involving 3D-printed anatomic models and 25 studies on surgical guides, which reported average time savings of 62 minutes (\$3,720 per case) and 23 minutes (\$1,488 per case), respectively. Using an average OR cost of \$62 per minute (ranging from \$22 to \$133), the study simulated different financial scenarios and concluded that producing 63 models or guides annually (approximately 1.2 per week) would cover fixed costs and break even. The results emphasize that, despite the resource demands, 3D-printed models and guides provide substantial long-term savings for healthcare systems, improving operational efficiency and reducing overall healthcare costs while also enhancing patient outcomes (30).

A systematic review by Liu et al. evaluates and compares the safety and efficacy of 3D navigation-assisted osteotomy versus conventional osteotomy for treating developmental dysplasia of the hip (DDH) in children. Of 626 initially identified studies from databases such as PubMed, Embase, and the Cochrane Library, seven retrospective

cohort studies involving 288 cases met the inclusion criteria. The meta-analysis revealed that 3D navigation-assisted osteotomy significantly reduced surgical duration, intraoperative bleeding, and radiation exposure compared to conventional methods. It also showed fewer cases of poor clinical function graded by McKay criteria. However, there were no significant differences between the two approaches in terms of corrected acetabular index angle, postoperative leg length discrepancy, or Severin x-ray outcomes. This study contributes to the literature by pointing out the benefits of using 3D navigation-assisted osteotomy to enhance the efficiency and safety of surgeries, while also recognizing opportunities for more investigation to improve long-term functional and imaging results for DDH in children (31).

Another study by Zhang et al. investigated the use of a 3D-printed multifunctional guide plate (3D-MGP) to improve surgical precision and outcomes in the treatment of benign tumors of the proximal femur. The study included 17 patients who underwent tumor curettage and implant fixation using a 3D-printed multifunctional guide plate designed using computer-aided techniques to ensure accurate tumor localization, controlled incisions, and precise screw placement. The surgeries achieved complete tumor resection without minor surgical complications, unintended incisions, or misplaced screws, demonstrating the reliability of the evidence in improving safety and precision. The mean operative time was 126.47 minutes, and the mean Musculoskeletal Tumor Society (MSTS) score was 27.29, indicating favourable functional outcomes at a median follow-up of 16.4 months. The results highlight the potential of 3D printing technology to customize surgical approaches, reduce operative times, intraoperative bleeding, and radiation exposure, and thus improve overall outcomes in orthopaedic surgical procedures (32).

In another retrospective study, Lagerborg evaluated the effectiveness of preoperative 3D planning and 3D-printed surgical guides, comparing the results of conventional osteotomies using the Imhauser technique performed between 2009 and 2013 with those using 3D-assisted surgeries performed between 2014 and 2021. The study focused primarily on improvements in hip range of motion (ROM), and secondary assessments included radiographic findings, patient-reported clinical outcomes, and operative duration. Although no significant improvements in hip range of motion were observed, the 3D imaging-assisted group demonstrated slightly better radiographic

findings and shorter operative duration. Statistical methods such as t-tests and Mann-Whitney U tests were used to analyse normally and non-normally distributed data, and parameters such as Southwick angle changes and patient-reported outcomes further supported the results (33).

Additionally, Moralido et al. examined the effectiveness of patient-specific (PS) osteotomy guides in improving the accuracy of femoral neck osteotomy during primary total hip replacement (THA). Using three-dimensional (3D) computed tomography (CT) analysis, the researchers evaluated the accuracy of PS guides in 103 THR cases by comparing pre- and postoperative CT data. Using 3D planning, the optimal osteotomy level was determined with the primary objective of assessing discrepancies between planned and actual osteotomy levels, while clinical outcomes were analysed as a secondary objective. The results showed a mean discrepancy of 0.3 mm (interquartile range: -1 mm to 2 mm) with a strong positive correlation between the planned and actual levels ($R^2 = 0.9$, $p < 0.001$) (34).

In summary, 3D printing has opened new opportunities for surgical planning and patient-specific instrumentation in orthopaedics, improving accuracy, efficiency, and clinical safety. However, its widespread clinical adoption remains limited due to high cost, complex workflows, and case-specific customization.

3. METHODOLOGY

This study was carried out according to the standard surgical steps of proximal femoral osteotomy described in earlier research (12, 37–40). Based on this, an experimental protocol was developed that included three stages: (1) the design and 3D printing of a standardized guide, (2) stepwise simulation trials on synthetic pediatric femur models, and (3) assessment of accuracy, operative time, and surgeon feedback through questionnaires. The findings were evaluated in relation to the planned correction values as well as previously published outcomes.

3.1 Surgical Guide Designing

The design and development of the surgical guide were carried out in collaboration with experienced orthopaedic surgeons. Initial discussions focused on identifying common intraoperative challenges, including wire alignment, angle control, and ergonomic limitations of existing instruments. These discussions were carefully recorded and used to inform the conceptualization of a hybrid design that combines the key features of traditional surgical instruments with the precision alignment advantages of patient-specific guides. Based on these discussions, a concept diagram was prepared to outline the main components. (Figure 3.1.).

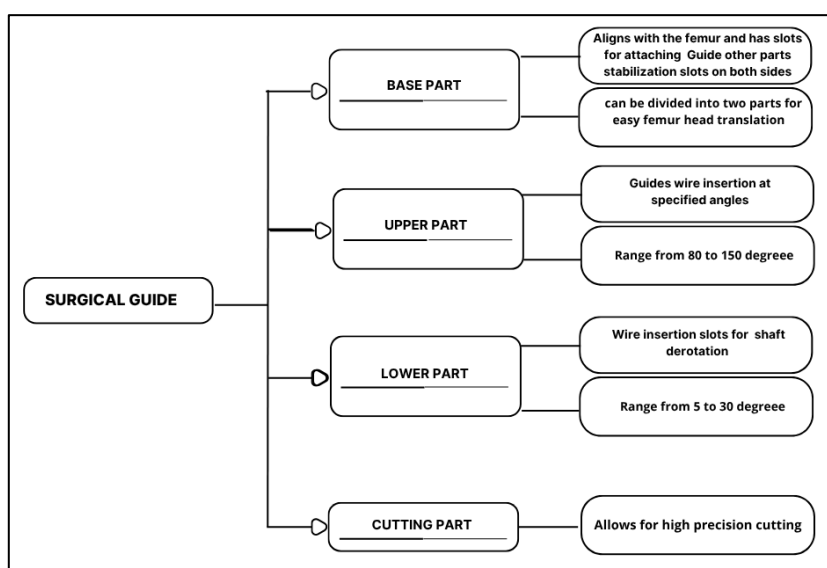


Figure 3. 1. Concept diagram of the hybrid design approach

The guide design was carried out using SolidWorks (Versions 2025, Dassault Systèmes, Vélizy-Villacoublay, France). It was designed with a modular structure to allow adjustments in angulation, rotation, and translation, either individually or in combination. These models highlighted important anatomical landmarks that helped determine the initial guide design. To define precise dimensions for the final device, actual measurements were then obtained from established biomechanical studies (35;36). The definitive design was created using averaged dimensions that balanced anatomical accuracy with the minimum requirements of the 3D printer, while also ensuring compatibility with the available experimental models. The initial design (Figure 3.2.) focused on ensuring compatibility with varied NSAs and anteversions seen in paediatric cases.

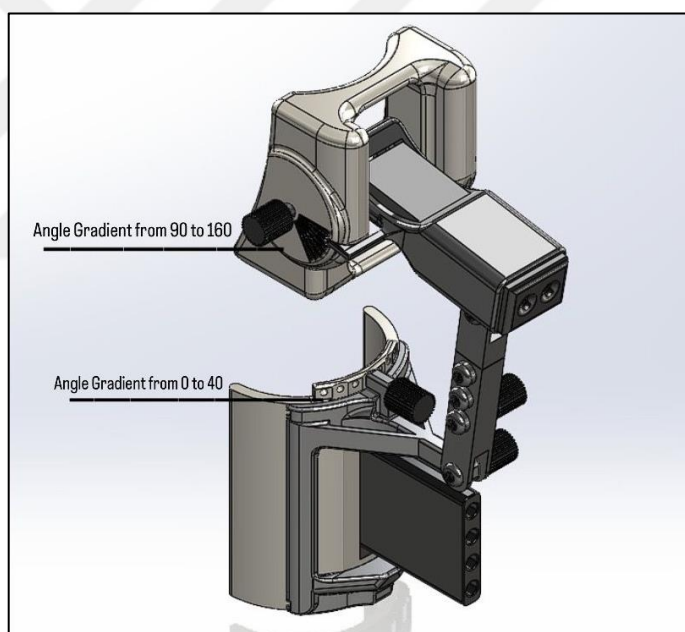


Figure 3. 2. Initial design of the guide

Preliminary evaluation of the prototype confirmed its ability to guide angular corrections with acceptable precision. The bridge mechanism allowed for controlled translation of the femoral head segment following osteotomy. However, testing showed limitations related to the complexity of assembly. In response, design revisions (Figure 3.3.) were undertaken with particular attention to rotational osteotomies. Modifications included improvements to the locking and stabilization mechanisms to maintain

positional alignment following osteotomy cuts, particularly during plate and screw fixation. These enhancements focused on the integration of interlocking components within the surgical guide that collectively ensured rigid fixation during drilling and cutting. The design also incorporated stabilization connectors to support precise guide placement. This design aimed to enhance intraoperative usability and mechanical stability.

The final design of the surgical guide consisted of four main parts, each serving a specific purpose. The base (Figure 3.3a) was reinforced to anchor the guide firmly to the femoral surface, ensuring a stable reference plane during osteotomy. Also, the base was divided into two parts connected by a modular joint to allow controlled translation. The upper part (Figure 3.3b) consisted of a base with an adjustable angle range from 80° to 150° , along with an angle pointer that allowed visualization and confirmation of the intended correction angle before cutting. A cutting modular (Figure 3.3c) was incorporated into the mid-section of the guide to direct the oscillating saw blade along predefined planes, minimizing variability during osteotomy execution. The lower part (Figure 3.3d) contained a K-wire slot, positioned to allow insertion at specific rotation angles, enabling control of torsional correction from the neutral midpoint (0°) up to 30° in either direction. Additionally, stabilization connectors (Figure 3.3e) were incorporated between the base components to secure them once aligned, ensuring mechanical stability during drilling and fixation as well as after completion of the osteotomy.

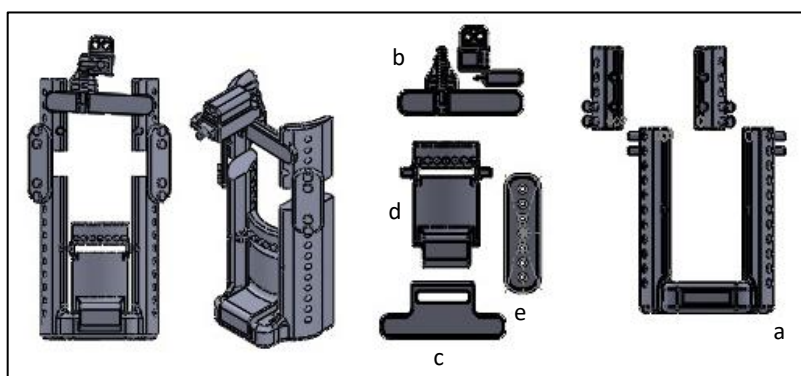


Figure 3. 3. Revised surgical guide model

3.2. Guide 3D Printing

After the final version selected (Figure 3.4.), two additive manufacturing techniques -fused deposition modeling (FDM) and stereolithography (SLA)- were considered to evaluate the mechanical integrity and engineering feasibility of the proposed standardized surgical guide.

While SLA was considered in initial comparisons for its superior surface finish (offering a minimum layer thickness of 0.02 mm and closer tolerances of ± 0.25 mm), the higher material and processing costs made it less suitable for iterative prototyping at this stage. Therefore, the pilot prototype was fabricated using FDM (Fused Deposition Modeling) technology with polylactic acid (PLA) filaments. This technology was selected due to its affordability, high dimensional consistency, and ease of post-processing. These features make FDM particularly suitable for repeatable testing, alignment verification, and mechanical evaluation under simulated surgical conditions. FDM supports layer thicknesses ranging from 0.05 to 0.3 mm, with a minimum feature size of 0.2 mm and a dimensional tolerance of $\pm 0.5\%$ (± 0.5 mm), providing sufficient accuracy for assessing key geometric features and structural performance (23,24).

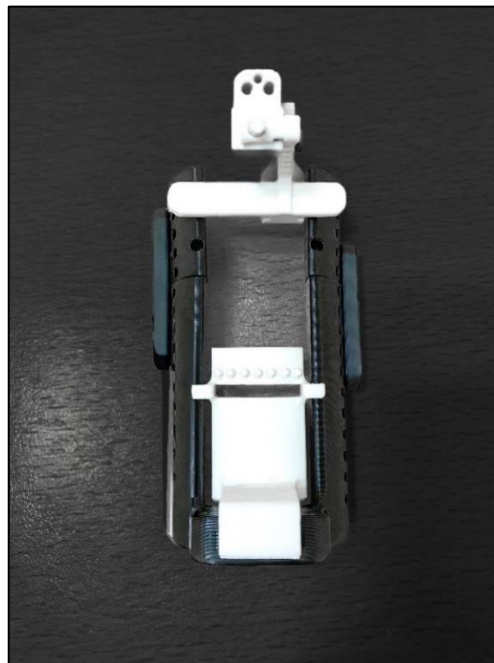


Figure 3. 4. 3D printed prototype surgical guide

3.3. Surgical Procedure

In this study, third-generation paediatric composite femur models (Silbons Research Laboratory, Kayseri, Turkey) were employed (Figure 3.5.). According to the manufacturer's technical specifications, these synthetic femora are capable of withstanding axial loads of up to 1532 N. These models are widely used in orthopaedic research due to their reproducible geometry and validated biomechanical properties, making them suitable for simulating paediatric femoral anatomy in experimental settings.



Figure 3. 5. Femur models

A total of five simulated proximal femoral osteotomies were conducted using the 3D-printed surgical guide. The experiments were organized into two sessions.

- **Session 1 (pilot trials):** Two procedures were performed without prior access to the user manual for the guide. One trial was conducted by a junior assistant surgeon and the other by a senior surgeon, in order to observe usability across different experience levels.
- **Session 2 (guided trials):** Three trials were conducted after participants had prior access to the user manual, which included labelled diagrams, explanatory notes, and a simulation video (Figure 3. 6.)

This session also featured a more realistic operative setup, to better replicate intraoperative conditions (Figure 3.6b). Four junior assistant surgeons participated in these trials.

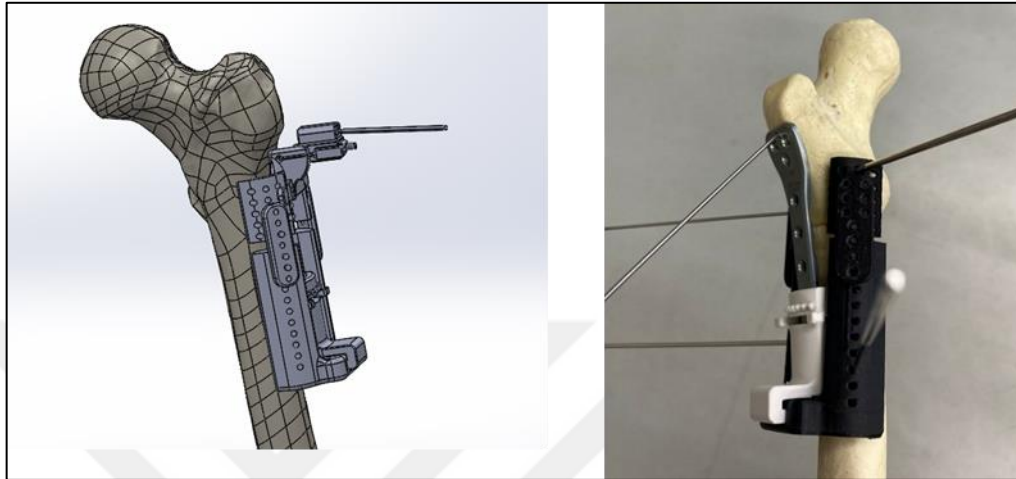


Figure 3. 7. Simulation of the guide on femur bone. a) in virtual environment. b) Prototype with LCP plate placed

After preoperative planning, the osteotomy axis and cutting level were marked on the bone model. The procedure began by inserting a reference K-wire through the designated hole in the upper part of the guide to establish the planned correction angle. Two additional wires were placed into the femoral head to guide proximal screw positioning. Once alignment was confirmed, the osteotomy cut was performed at the marked level using a B.S.F Motors TR-X Series orthopedic surgical drill and oscillating saw.

The lower part of the guide was then used to adjust the anteversion/retroversion angle according to the preoperative plan. Additional stabilization was achieved by inserting lateral K-wires (two on either side of the upper and lower base parts). After correction, the guide middle parts were removed, and the proximal femur fragment was fixed with a 3.5 mm Locking Compression Plate (LCP). The preoperative measurements, planned correction angles, fixation plate, and rotation adjustments for each simulated case are summarized in Table 3.1.

Table 3. 1. Preoperative planning and LCP plate selection for experimental cases

| Case | Pre-op NSA (°) | Planned Correction (°) | Plate Used | Rotation Correction |
|-------------|-----------------------|-------------------------------|-------------------|----------------------------|
| 1 | 147 Coxa valga | Varus 17 | 110° LCP | 19° |
| 2 | 151 Coxa valga | Varus 21 | 110° LCP | 14° |
| 3 | 106 Coxa vara | Valgus 24 | 150° LCP | 6° |
| 4 | 111 Coxa vara | Valgus 19 | 150° LCP | 11° |
| 5 | 142 Coxa valga | Varus 12 | 120° LCP | 12° |

Upon completion of all simulations, a structured questionnaire was distributed to the participating surgeons to evaluate usability, accuracy, ergonomics, and overall performance of the guide. The collected feedback was essential for assessing surgeon satisfaction, validating clinical usability, and identifying areas for iterative improvement.

4. RESULTS

This section reports the outcomes of five simulated proximal femoral osteotomy procedures performed using the developed 3D-printed standardized surgical guide. The evaluation was designed to assess the guide's performance in achieving precise correction of angulation and rotation. Translation was assessed as a secondary outcome to provide additional insight into alignment accuracy. Furthermore, operative duration, number of Kirschner wires (K-wires) required, and intraoperative handling characteristics were systematically recorded to evaluate the practicality and usability of the device.

To assess the accuracy of osteotomy correction, measurements were performed using both manual and digital methods. For angulation, the neck–shaft angle (NSA) was determined on standardized AP views by marking the femoral shaft axis and the neck axis, and measuring the angle between them with a goniometer. For digital analysis, standardized photographs of the models were obtained, and angles were measured using an angle-measuring application. Rotation was measured using a reference K-wire inserted perpendicular to the shaft axis distal to the osteotomy and a second K-wire aligned with the femoral neck axis; the angle between the two wires was recorded. Changes between the planned and achieved orientations were calculated to determine rotational accuracy. Translation was assessed as a secondary outcome by measuring the linear offset at the osteotomy level between the planned and achieved fragment positions. Measurements were obtained in two representative cases, where preoperative offsets of 18 mm and 20 mm were reduced to postoperative residual errors of 1.2 mm and 0.9 mm, respectively. Each measurement was repeated three times and averaged, and deviations from the planned corrections were reported as the correction error (Table 4.1.).

Table 4. 1. Preoperative deformity and postoperative residual error.

| Trial | Angulation (degrees) | | Rotation (degrees) | |
|----------------|------------------------|-------------------------|------------------------|-------------------------|
| | Pre-operative vs. Plan | Post-operative vs. Plan | Pre-operative vs. Plan | Post-operative vs. Plan |
| 1 | 17 | 2 | 19 | 2 |
| 2 | 21 | 1.5 | 14 | 0 |
| 3 | 24 | 1 | 6 | 0 |
| 4 | 19 | 0 | 11 | 1 |
| 5 | 12 | 1.8 | 12 | 1.7 |
| Average | 18.6 | 1.26 | 12.4 | 0.94 |

Across all trials, the surgical guide demonstrated high accuracy in achieving the planned corrections. The mean preoperative angulation error was $18.6^\circ \pm 4.51$, which was reduced to $1.26^\circ \pm 0.80$ postoperatively. Similarly, the mean rotational error decreased from $12.4^\circ \pm 4.72$ preoperatively to $0.94^\circ \pm 0.93$ postoperatively. Paired t-test analysis confirmed that these reductions in both angulation ($t = 7.92, p = 0.0014$) and rotation ($t = 6.11, p = 0.0036$) were statistically significant. These findings validate the guide's ability to provide precise and reproducible correction of proximal femoral deformities in simulated paediatric models.

To examine the effect of user experience on performance, all trials were distributed across different sessions. This design allowed observation of trends in procedural time and guide handling across sessions (Figure 4.1.). Procedural duration decreased across the first four cases, ranging from 16 minutes in the first trial to 11 minutes in the fourth, before increasing slightly to 13 minutes in the fifth. The number of K-wires used remained consistent, varying between 6 and 7 across all trials.

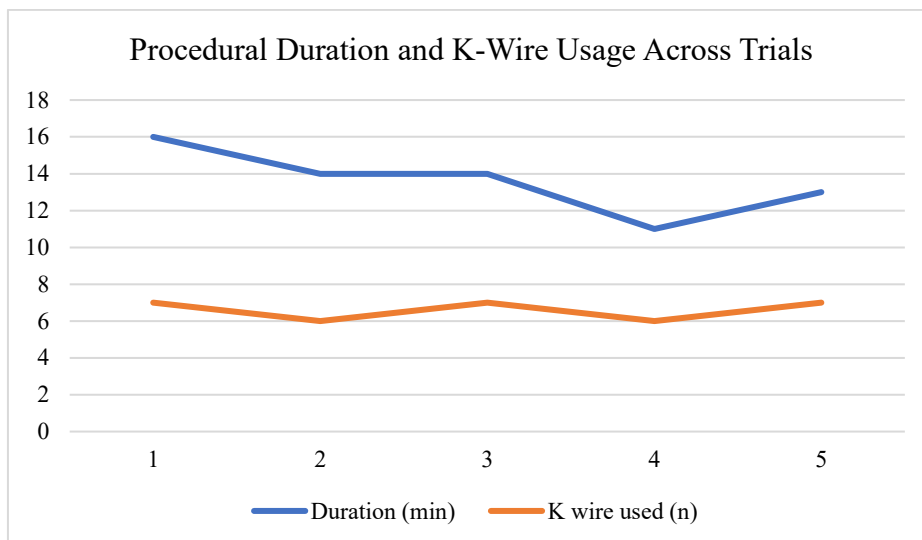


Figure 4. 1. Procedural duration and K-wire usage across trials

The mean usability scores of the standardized surgical guide ranged between 2.2 and 4.6 on a five-point scale (1 = very difficult, 5 = very easy). The overall functionality of the device was rated highest, with a mean of (4.6 ± 0.89), followed by the accuracy of the angulation and rotation component (4.2 ± 0.45). The guide's role in minimizing operative time was also rated favourably (3.8 ± 0.84), as was the ease of K-wire slot usage (3.6 ± 0.55). Placement of the device on the bone achieved a moderate rating (2.8 ± 0.84), while the stabilization component showed a similar moderate level (3.0 ± 0.71). In contrast, the functionality of the base and connector received the lowest evaluation (2.2 ± 0.84).

5. DISCUSSION

This research focused on the development of a 3D-printed standardized surgical guide as an alternative to patient-specific guides in paediatric proximal femoral osteotomy. The guide was designed to provide precise surgical angulation and rotation, while also enabling improved fixation for implant placement within the bone. Most current research emphasizes patient-specific surgical guides and their clinical benefits [42–46], the broader findings reported by Macanina et al. (40) including improved osteotomy accuracy, and reduced operative time, highlight the value of adaptable design principles. Although the surgical guide developed in this study is standardized rather than patient-specific, it incorporates modular components to accommodate anatomical variability in paediatric patients, combining the precision typically associated with customized solutions with the scalability of a standardized system.

Functional evaluation confirmed the guide's effectiveness, with angulation and rotation correction rated at 4.2 ± 0.45 . The achieved postoperative alignment deviated on average by $1.26^\circ \pm 0.80$ for angulation and $0.94^\circ \pm 0.93^\circ$ for rotation. Relative to previously reported outcomes, Assink et al. (38) reported deviations of $2.1 \pm 1.0^\circ$ for angulation and $3.4 \pm 1.6^\circ$ for rotation, while Neopoulos et al. (48) reported $2.4^\circ \pm 1.9^\circ$ for femoral torsion. It should be noted, however, that the sample size, experimental environment, and osteotomy types differed from those in the referenced studies; therefore, these comparisons should be interpreted cautiously. Performance across multiple cases demonstrated reproducible outcomes, directly supporting the hypothesis that the same guide can be reliably applied across different pediatric femoral morphologies. Questionnaire responses confirmed this reproducibility, with uniformly high ratings for overall functionality 4.6 ± 0.89 , and procedural times stabilized after initial trials (Figure 4.1). The inclusion of a user manual facilitated understanding of optimal device use, and surgeon feedback highlighted specific strengths of the design: the lower part was particularly effective for rotational orientation, while the upper part supported consistent osteotomy alignment.

Compared to previous studies, our results indicate notable procedural efficiency. In the present study, the mean time required per Kirschner wire was 1.8 minutes, which is lower than the 2.1 minutes reported for 3D-printed customized guides by Duan et al. (47) where the experimental group achieved a significant reduction in wire placement

time compared to the control group (4.6 minutes vs. 2.1 minutes), underscoring the operative advantage offered by 3D-printed navigation. It should be noted, however, that differences in the experimental environment and the nature of the specimens used may have influenced the observed time per wire, so direct comparisons should be interpreted cautiously. The initial trials demonstrated a brief learning curve in applying the surgical guide; subsequent uses revealed enhanced efficiency and ease of use, with operative time decreasing from 16 minutes in the first trial to 11 minutes by the fourth, after which times stabilized. No significant differences in device handling or correction accuracy were observed between senior and junior surgeons, suggesting that the guide can be effectively adopted regardless of experience level. These results highlight how important it is to integrate preoperative training or simulation into clinical processes when introducing new surgical instruments (51), as even limited training was sufficient to achieve efficiency and confidence in use.

The findings of this research align with broader evidence on the value of standardization in surgical practice. A study by pai et al. (41) demonstrated that structured curricula that encourage the use of standardized tools increase cost-effectiveness, preserve surgical autonomy, and improve overall operating room performance. Although focused on general surgical procedures, the core principle, that standardization can reduce variability and improve surgical outcomes, is directly relevant to the development of standardized guides in orthopaedic surgery. Applying these principles to paediatric femur osteotomy improves procedural consistency, supports surgical training, and contributes to safer and more reproducible outcomes. This reinforces the argument for integrating standardized tools within paediatric orthopaedic workflows as a means to balance efficiency, precision, and safety. In the current study, a fixed-segment splint system was used to maintain alignment between the femoral shaft and head after osteotomy. However, surgeon observations highlighted limitations in cases requiring extensive posterior repositioning of the femoral head due to the fixed design. To address this, a connector was added and the splint was separated, enabling femoral head translation across multiple planes. These modifications were reflected in the usability outcomes: while overall functionality received high ratings 4.6 ± 0.89 , the base/connector 2.2 ± 0.84 achieved only moderate to low scores, underscoring the challenges in achieving both flexibility and stability within the splint prototype.

The current cutting guide model demonstrated the required accuracy during trials on paediatric femur models; however, slight vertical movement of the sawblade was observed in some cases due to the thickness of the cutting slot. This observation aligns with the findings of Kwan et al., (39) who identified that a jig thickness of 15 mm and a slot height of 100–120% of the sawblade width provide an optimal balance between cutting accuracy and surgical practicality. Therefore, incorporating these findings into the final design, especially when producing the guide with suitable metallic materials, will involve narrowing the cutting slot and potentially adding adjustable angular features to enhance control, reduce vertical deviation, and improve the guide's surgical performance in paediatric femoral osteotomies.

At the same time, challenges with stability due to the multi-part nature of the guide, previously reflected in lower ratings for stabilization 3.0 ± 0.71 and the base/connector 2.2 ± 0.84 , were reiterated here. These difficulties were compounded by the open experimental environment, which does not fully replicate clinical conditions where the femur is fixed and surrounded by soft tissues. Although the detachable section allowed translation, maintaining stability once the connectors were removed remained difficult under the test conditions. Taken together, these findings address the hypothesis on ergonomics and ease of use, suggesting that while the device is highly effective in accuracy and alignment, refinements are required to improve intraoperative stability and handling.

Although our results are promising, given that the trials were limited by their small sample size, generalizability may be difficult. This observation is consistent with the findings of Sun et al. (27), who noted that the small sample size may impair the ability to detect significant differences and may not reflect the diversity of deformities in general clinical practice. Furthermore, the fact that trials were performed by assistant surgeons may have influenced the results, as this experience may not be representative of the average level of performance in a typical clinical setting (49). Therefore, this study suggests future research on larger and more diverse patient groups, involving multiple surgeons with different experience levels, to ensure greater accuracy.

The results of this thesis should be interpreted with caution, as their accuracy is inherently limited. All corrections and measurements were performed on physical 3D-printed bone models and further evaluated through two-dimensional images rather than

in a true surgical environment. This limitation in method implies that the reported angulation, rotation, and translation values may not precisely reflect what would be achieved in vivo. In particular, the absence of three-dimensional imaging reduces data reliability (50). Moreover, the results were reported as averages across a small number of trials, and the limited sample size restricted the ability to perform robust statistical analysis. Future studies employing larger datasets, three-dimensional assessment tools, and application in real surgical cases are required to validate and refine these findings.

The efficiency achieved with our standardized guide suggests that modular standardized designs may reach performance levels comparable to customized solutions, while offering greater scalability, practicality, and potential for broader clinical adoption. Looking forward, the next versions of the device should be produced using finalized anatomical dimensions and constructed from biocompatible, sterilizable medical-grade materials such as PEEK or surgical stainless steel. In addition, while the current dimensions were designed to be broadly applicable across paediatric femoral geometries, future iterations may be manufactured in standardized size categories (e.g., small, medium, large) to better accommodate variability in bone morphology across patients. Future designs should also aim to reduce the number of separate components, thereby improving ease of handling, setup efficiency, and intraoperative stability without compromising functionality.

6. CONCLUSION AND FUTURE STUDIES

This study introduced the design and preliminary validation of a standardized modular surgical guide for proximal femoral osteotomy in paediatric cases. The findings demonstrated that the guide achieved accurate correction of femoral anteversion and neck–shaft angle, with reproducible outcomes across different femoral morphologies. Trials conducted by assistant surgeons showed that the device could be used with confidence and high accuracy even by less experienced operators. The mean time per Kirschner wire was 1.8 minutes, indicating efficiency comparable to specific guides reported in the literature, while usability ratings confirmed strong performance in alignment and rotational accuracy. Although stability of the connector and base components requires refinement, the results collectively support the hypotheses that a standardized 3D-printed guide can provide precision, reproducibility, and usability in paediatric osteotomy.

Nevertheless, the evaluation was limited to a small number of simulated procedures using non-medical, scaled experimental materials, which were chosen to facilitate fabrication and handling during the preliminary phase. Future research should focus on validation through clinical tests that include a wider range of femoral morphologies and deformities. It will also be necessary to adopt sterilizable, biocompatible materials suitable for surgical environments and to refine ergonomic features to enhance intraoperative usability. Comparative studies against conventional osteotomy techniques, long-term performance assessments, and multicentre evaluations by orthopaedic surgeons will be critical for establishing clinical effectiveness and enabling broader adoption of the guide.

REFERENCES

1. Dance, S., Quan, T., Parel, P., Farley, B., & Tabaie, S. A. (2024). Pediatric Hip Dysplasia Surgery Outcomes by Pediatric Versus Nonpediatric Orthopedists. *Cureus*, *16*. <https://doi.org/10.7759/cureus.55951>
2. Barlow, B. T., Bittersohl, B., Schmitz, M. R., & Hosalkar, H. S. (2014). *Proximal Femoral Osteotomies in Residual Childhood Disease*. https://link.springer.com/content/pdf/10.1007%2F978-1-4614-7321-3_39-1.pdf
3. Mifsud, M., Buckingham, R., & Theologis, T. (2021). Planning a proximal femoral varus osteotomy in paediatric orthopaedics. *Techniques in Orthopaedics*, *36*(2), 157–161. <https://doi.org/10.1097/BTO.0000000000000422>
4. Zakani, S., Chapman, C., Saule, A., Cooper, A., Mulpuri, K., & Wilson, D. R. (2021). *Computer-assisted subcapital correction osteotomy in slipped capital femoral epiphysis using individualized drill templates*. *7*(1), 18. <https://doi.org/10.1186/S41205-021-00108-6>
5. Nagpure, D., & Asutkar, S. (2024). 3D Printing in Surgery: Transforming Patient-Specific Solutions. *Multidisciplinary Reviews*, *8*(5), 2025154. <https://doi.org/10.31893/multirev.2025154>
6. Hedequist, D. J., & Heyworth, B. E. (2018). *Paediatric femur fractures: A practical guide to evaluation and management* (pp. 6–21). Springer US. <https://doi.org/10.1007/978-3-319-63245-3>
7. Singh, I. (2011). *Textbook of anatomy: Volume 1: Upper extremity, lower extremity*. Jaypee Brothers Medical Publishers Pvt. Limited. https://www.google.com.tr/books/edition/Textbook_of_Anatomy/YP5I30Rrk3IC
8. Byrne, D. P., Mulhall, K. J., & Baker, J. F. (2010). Anatomy & biomechanics of the hip. *The Open Sports Medicine Journal*, *4*(1), 51–57. <https://doi.org/10.2174/1874387001004010051>
9. Babhulkar, S., & Tanna, D. (2013). *Proximal femoral fractures*. Jaypee Brothers Medical Publishers Pvt. Limited. https://www.google.com.tr/books/edition/Proximal_Femoral_Fractures/kVIEO7nIIHUC
10. Jouve, J.-L., Glard, Y., Garron, E., Piercecchi, M.-D., Dutour, O., Tardieu, C., & Bollini, G. (2005). Anatomical study of the proximal femur in the fetus. *Journal of Pediatric Orthopaedics B*, *14*(2), 105–110. <https://doi.org/10.1097/01202412-200503000-00007>
11. Ibrahim. (2015). Tachdjian's paediatric orthopaedics: From the Texas Scottish Rite Hospital for Children [Review of the book *Tachdjian's paediatric orthopaedics*]. *Malaysian Orthopaedic Journal*, *9*(1), 53. <https://doi.org/10.5704/MOJ.1503.012>

12. M'sabah, D. L., Assi, C., & Cottalorda, J. (2013). Proximal femoral osteotomies in children. *Orthopaedics & Traumatology: Surgery & Research*, 99(Suppl. 1), S171–S186. <https://doi.org/10.1016/j.otsr.2013.07.002>
13. Herring, J. A. (2007). *Tachdjian's paediatric orthopaedics: From the Texas Scottish Rite Hospital for Children* (4th ed.). Saunders Elsevier.
14. Mast, J. W. (2018). Generic preoperative planning for proximal femoral osteotomy in femoral neck nonunion. *Orthopaedics*, 41(1), e1–e6. <https://doi.org/10.3928/01477447-20171220-01>
15. Zhou, W., Guo, H., Duan, R., & Shi, Q. (2022). Visualized simulative surgery in preoperative planning for proximal femoral varus osteotomy of DDH. *BMC Musculoskeletal Disorders*, 23, 295. <https://doi.org/10.1186/s12891-022-05219-7>
16. Sezgin, E. A., Akgün, R. C., Öztürk, K., Kalenderer, Ö., & Agus, H. (2023). Comparison of the radiological and clinical results of femoral varus osteotomy in patients with Legg–Calvé–Perthes disease. *Acta Orthopaedica et Traumatologica Turcica*, 57(1), 42–46. <https://doi.org/10.1016/j.aott.2019.01.002>
17. Otani, T., Whiteside, L. A., & White, S. E. (1993). Cutting errors in preparation of femoral components in total knee arthroplasty. *The Journal of Arthroplasty*, 8(5), 503–510. [https://doi.org/10.1016/S0883-5403\(06\)80031-7](https://doi.org/10.1016/S0883-5403(06)80031-7)
18. Deshpande, S. S. (2024). Osteotomy wedge angle – Aiming to achieve perfection with new device: Pre-clinical stage. *Journal of Clinical Orthopaedics and Trauma*, 54, 102474. <https://doi.org/10.1016/j.jcot.2024.102474>
19. Sys, G., Eykens, H., Lenaerts, G., Shumelinsky, F., Robbrecht, C., & Poffyn, B. (2017). Accuracy assessment of surgical planning and three-dimensional-printed patient-specific guides for orthopaedic osteotomies. *Proceedings of the Institution of Mechanical Engineers, Part H: Journal of Engineering in Medicine*, 231(6), 499–508. <https://doi.org/10.1177/0954411917702177>
20. Fan, X., Zhu, Q., Tu, P., Joskowicz, L., & Chen, X. (2023). A review of advances in image-guided orthopaedic surgery. *Physics in Medicine & Biology*, 68(2), 02TR01. <https://doi.org/10.1088/1361-6560/aca9>
21. Rodriguez Colon, R., Nayak, V. V., Parente, P. E. L., Leucht, P., Tovar, N., Lin, C. C., Rezzadeh, K., Hacquebord, J. H., Coelho, P. G., & Witek, L. (2023). The presence of 3D printing in orthopaedics: A clinical and material review. *Journal of Orthopaedic Research*, 41(3), 601–613. <https://doi.org/10.1002/jor.25388>
22. Dong, C., Petrovic, M., & Davies, I. J. (2024). Applications of 3D printing in medicine: A review. *Annals of 3D Printing in Medicine*, 14, 100149. <https://doi.org/10.1016/j.stlm.2024.100149>
23. Chen, H. J., & Gariel, M. (2012). *A roadmap from idea to implementation: 3D printing for pre-surgical applications* (1st ed.). CreateSpace Independent Publishing Platform.

24. Aimar, A., Palermo, A., & Innocenti, B. (2019). The role of 3D printing in medical applications: A state of the art. *Journal of Healthcare Engineering*, 2019, 5340616. <https://doi.org/10.1155/2019/5340616>
25. Valchanov, P., & Ivanov, S. (2024). 3D printed anatomical models for preoperative planning of complex orthopaedic surgical operations of the lower limb. *Archives of Materials Science and Engineering*. <https://doi.org/10.5604/01.3001.0054.7401>
26. Gauci, M. O. (2022). Patient-specific guides in orthopaedic surgery. *Orthopaedics & Traumatology: Surgery & Research*, 108(1), 103154. <https://doi.org/10.1016/j.otsr.2021.103154>
27. Sun, J., Mu, Y., Cui, Y., Qu, J., & Lian, F. (2023). Application of 3D-printed osteotomy guide plates in proximal femoral osteotomy for DDH in children: A retrospective study. *Journal of Orthopaedic Surgery and Research*, 18(1), 315. <https://doi.org/10.1186/s13018-023-03801-w>
28. Zheng, P., Xu, P., Yao, Q., Tang, K., & Lou, Y. (2017). 3D-printed navigation template in proximal femoral osteotomy for older children with developmental dysplasia of the hip. *Scientific Reports*, 7, 44993. <https://doi.org/10.1038/srep44993>
29. Shi, Q., & Sun, D. (2020). Efficacy and safety of a novel personalized navigation template in proximal femoral corrective osteotomy for the treatment of DDH. *Journal of Orthopaedic Surgery and Research*, 15(1), 317. <https://doi.org/10.1186/s13018-020-01843-y>
30. Ballard, D. H., Mills, P., Duszak, R., Weisman, J. A., Rybicki, F. J., & Woodard, P. K. (2020). Medical 3D printing cost-savings in orthopaedic and maxillofacial surgery: Cost analysis of operating room time saved with 3D printed anatomic models and surgical guides. *Academic Radiology*, 27(8), 1103–1113. <https://doi.org/10.1016/j.acra.2019.08.011>
31. Liu, Y., Yang, Y., & Ding, S. (2022). Application of 3D navigation for osteotomy of DDH in children: A systematic review and meta-analysis. *Frontiers in Pediatrics*, 10, 1021981. <https://doi.org/10.3389/fped.2022.1021981>
32. Zhang, Y., Guo, Y., Li, Z., Wang, B., & Li, Z. (2024). 3D-printed multifunctional guide plate for fenestration and screws drill in proximal femoral benign tumor. *Orthopaedic Surgery*, 16(6), 1487–1492. <https://doi.org/10.1111/os.14075>
33. Lagerburg, V., van den Boorn, M., Vorrink, S., et al. (2024). The clinical value of preoperative 3D planning and 3D surgical guides for Imhäuser osteotomy in slipped capital femoral epiphysis: A retrospective study. *3D Printing in Medicine*, 10(8). <https://doi.org/10.1186/s41205-024-00205-2>
34. Moralidou, M., Di Laura, A., Henckel, J., Hothi, H., & Hart, A. J. (2022). Accuracy of a three-dimensional (3D)-printed patient-specific femoral osteotomy guide: A computed tomography study. *Bioengineering*, 9(11), 667. <https://doi.org/10.3390/bioengineering9110667>

35. Szuper, K., Schlégl, Á. T., Leidecker, E., Vermes, C., Somoskeöy, S., & Than, P. (2015). Three-dimensional quantitative analysis of the proximal femur and the pelvis in children and adolescents using an upright biplanar slot-scanning X-ray system. *Pediatric Radiology*, *45*(3), 411–421. <https://doi.org/10.1007/s00247-014-3146-2>
36. Yurtgün, M. F. (2014). *Pediatric femur cisim kırığının titanyum elastik çivi ile tedavisi: Radyolojik ve klinik değerlendirme* (Uzmanlık tezi, Selçuk Üniversitesi). Ulusal Tez Merkezi.
37. Benady, A., Gortzak, Y., Ovadia, D., Golden, E., Sigal, A., Taylor, L. A., Paranjape, C., Solomon, D., & Gigi, R. (2025). Advancements and applications of 3D printing in paediatric orthopaedics: A comprehensive review. *Journal of Children's Orthopaedics*, *19*(2), 119–138. <https://doi.org/10.1177/18632521251318552>
38. Assink, N., Meesters, A. M. L., Ten Duis, K., Harbers, J. S., IJpma, F. F. A., van der Veen, H. C., Doornberg, J. N., Pijpker, P. A. J., & Kraeima, J. (2022). A two-step approach for 3D-guided patient-specific corrective limb osteotomies. *Journal of Personalized Medicine*, *12*(9), 1458. <https://doi.org/10.3390/jpm12091458>
39. Kwan, Y. H., Owyang, D., Ho, S. W. L., & Yam, M. G. J. (2023). 3D-printed patient-specific surgical guides: Balancing accuracy with practicality. *Journal of Clinical Orthopaedics and Trauma*, *46*, 102293. <https://doi.org/10.1016/j.jcot.2023.102293>
40. McAnena, A. P., McClennen, T., & Zheng, H. (2025). Patient-specific 3-dimensional-printed orthopedic implants and surgical devices are potential alternatives to conventional technology but require additional characterization. *Clinical Orthopaedic Surgery*, *17*(1), 1–15. <https://doi.org/10.4055/cios23294>
41. Pei, K. Y., Richmond, R., & Disanaïke, S. (2020). Surgical instrument standardization: A pilot cost consciousness curriculum for surgery residents. *American Journal of Surgery*, *219*(2), 295–298. <https://doi.org/10.1016/j.amjsurg.2019.10.018>
42. Xu, J., Xu, J., Xie, K., Hu, X., Wu, H., Gao, L., Wang, L., & Yan, M. (2021). Using a patient-specific 3D-printed surgical guide for high tibial osteotomy: A technical note. *Journal of Shanghai Jiaotong University (Science)*, *26*(3), 339–345. <https://doi.org/10.1007/s12204-021-2302-8>
43. Nasti, S., Anjum, S., Kalekhan, S. M., Ashok, A. B., Bumb, P. P., & Puthenkandathil, R. (2023). Surgical guides: Precision redefined in implant placement. *IP International Journal of Periodontology and Implantology*, *8*(4), 177–180. <https://doi.org/10.18231/j.ijpi.2023.035>

44. Oldhoff, M. G. E., Posada-Álvarez, C., ten Duis, K., Doornberg, J. N., Assink, N., & IJpma, F. F. A. (2025). Patient-specific implants combined with 3D-printed drilling guides for corrective osteotomies of multiplanar tibial and femoral shaft malunions leads to more accurate corrections. *European Journal of Trauma and Emergency Surgery*, *51*(1), 1–11. <https://doi.org/10.1007/s00068-024-02755-w>
45. Bishop, M., Zaffagnini, S., Grassi, A., Dal Fabbro, G., Smyrl, G., Roberts, S., & MacLeod, A. (2023). Patient-specific distal femoral osteotomy reduces surgical time: Demonstration of a novel patient-specific technique. *Orthopaedic Proceedings*, *105*(16), 54. <https://doi.org/10.1302/1358-992X.2023.16.054>
46. Moralidou, M., Henckel, J., Di Laura, A., & Hart, A. (2023). Guiding prosthetic femoral version using 3D-printed patient-specific instrumentation (PSI): A pilot study. *3D Printing in Medicine*, *9*(1), 1–9. <https://doi.org/10.1186/s41205-023-00168-w>
47. Duan, X., Fan, H., Wang, F., Peng, H., & Yang, L. (2019). Application of 3D-printed Customized Guides in Subtalar Joint Arthrodesis. *Orthopaedic Surgery*, *11*(3), 405–413. <https://doi.org/10.1111/OS.12464>
48. Neopoulos, G., Jud, L., Vlachopoulos, L., & Fucntese, S. F. (n.d.). *Combined Correction of Coronal and Rotational Deformities of the Femur with Distal Femoral Osteotomy Using Patient-Specific Instrumentation*. <https://doi.org/10.1177/03635465251314868>
49. Jones, D. S. (2018). *Surgery and Clinical Trials: The History and Controversies of Surgical Evidence* (pp. 479–501). Palgrave Macmillan, London. https://doi.org/10.1057/978-1-349-95260-1_23
50. Liu, Z. (2006). AEstablishment of three-dimensional finite element model of proximal femur based on CT scan data. *Information of Medical Equipment*.
51. Bernier, G. V., & Sanchez, J. E. (2016). Surgical simulation: the value of individualization. *Surgical Endoscopy and Other Interventional Techniques*, *30*(8), 3191–3197. <https://doi.org/10.1007/S00464-016-5021-8>

THE FIRST PAGE OF THE PLAGIARISMREPORT

PROKSİMAL FEMORAL OSTEOTOMİ İÇİN 3D BASKILI STANDART CERRAHİ REHBERİN TASARIMI

ORJİNALLİK RAPORU

| | | | |
|----------------------------------|------------------------------------|-------------------------|--------------------------------|
| % 15 BENZERLİK ENDEKSİ | % 13 İNTERNET KAYNAKLARI | % 11 YAYINLAR | % 5 ÖĞRENCİ ÖDEVLERİ |
|----------------------------------|------------------------------------|-------------------------|--------------------------------|

BİRİNCİL KAYNAKLAR

| | | |
|-----------|---|-------------|
| 1 | www.hindawi.com İnternet Kaynağı | % 1 |
| 2 | www.researchgate.net İnternet Kaynağı | % 1 |
| 3 | lirias.kuleuven.be İnternet Kaynağı | % 1 |
| 4 | cdn.istanbul.edu.tr İnternet Kaynağı | % 1 |
| 5 | "The Pediatric and Adolescent Hip", Springer Science and Business Media LLC, 2019 Yayın | % 1 |
| 6 | www.science.gov İnternet Kaynağı | <% 1 |
| 7 | iopscience.iop.org İnternet Kaynağı | <% 1 |
| 8 | link.springer.com İnternet Kaynağı | <% 1 |
| 9 | www.mdpi.com İnternet Kaynağı | <% 1 |
| 10 | Submitted to Felician College Öğrenci Ödevi | <% 1 |
| 11 | www.coursehero.com İnternet Kaynağı | <% 1 |
| 12 | www.researchsquare.com İnternet Kaynağı | <% 1 |